Optical Materials 96 (2019) 109305

Contents lists available at ScienceDirect

Optical Materials

journal homepage: www.elsevier.com/locate/optmat

Broadband femtosecond nonlinear optical properties of silver nanowire films

Rambabu Allu[a], Dipanjan Banerjee[a], Ravikiran Avasarala[a], Syed Hamad[b], S. Venugopal Rao[c,**], G Krishna Podagatlapalli[a,*]

[a] Department of Electronics & Physics, GIS, GITAM deemed to be University, Visakhapatnam, 530045, Andhra Pradesh, India
[b] The Guo China –US Photonics Laboratory, State Key Laboratory of Applied Optics, Changchun Institute of Optics, Fine Mechanics and Physics, Chinese Academy of Sciences, Changchun, 130033, China
[c] Advanced Centre of Research in High Energy Materials (ACRHEM), University of Hyderabad, Hyderabad, 500046, Telangana, India

ARTICLE INFO

Keywords:
Silver nanowires
Saturable absorption
Reverse saturable absorption
Z-Scan

ABSTRACT

In this report, we present results from the investigation of femtosecond (fs) nonlinear optical (NLO) behaviour of silver nanowires (Ag NWs) films. High quality Ag NWs (10 μm length, diameter 50 nm in isopropyl alcohol) were utilzied for the NLO studies employing the standard Z-scan technique in both open and closed aperture configurations at wavelengths of 700 nm, 750 nm, 800 nm, 850 nm, 900 nm, and the corresponding NLO coefficients were estimated from theoretical fits to the experimental data. Nonlinear absorption in the Ag NWs at 800 nm demonstrated a pure reverse saturable absorption (RSA) with a strong two-photon absorption (TPA) coefficient. At 800 nm, intensity dependent Z-scan studies were performed at different peak intensities of 190 MW/cm^2, 210 MW/cm^2, 260 MW/cm^2 and observed that the TPA coeffieicent ($\sim 10^{-5}$ cm/W) increased significantly as a function of peak intensity. Interestingly, the nonlinear absorption of Ag NWs films demonstrated a complex behavior of saturable absorption (SA), reverse saturable absorption (RSA) and switching from RSA within SA depending on excitation wavelength even though the studies were performed at similar peak intensities. The estimated NLO coefficients were $I_S = 30$ MW/cm^2 ($\beta_{sa} = 0$), $\beta_{TPA} = 1.6 \times 10^{-5}$ cm/W, $I_S = 92$ MW/cm^2 ($\beta_{eff} = 1.4 \times 10^{-5}$ cm/W) and $I_S = 60$ MW/cm^2 ($\beta_{sa} = 1.72 \times 10^{-5}$ cm/W) for the wavelengths of 700 nm, 750 nm, 850 nm and 900 nm, respectively. The nonlinear refraction studies at the wavelength 800 nm, investigated by closed aperture Z-scan, demonstrated a positive sign (compared to the studies at other wavelengths) and the obtained intensity dependent nonlinear refractive index was $\sim 1.6 \times 10^{-9}$ cm^2/W.

1. Introduction

Optical data storage, optical information processing, optical limiting, optical switching, and image processing have emerged as a class of important technologies those predominantly depend on the nonlinear optical (NLO) properties exhibited by nanomaterials in general, and Plasmonic nanomaterials, in particular [1–6]. Plasmonic nanomaterials with different shapes afford unique challenge in appraising the structural morphology–NLO property relationship because of the formation of combined surface Plasmon resonances i.e. hotspots resulting from the nanomaterials when they are placed contiguously. In optical limiting studies, morphology of Plasmonic nanomaterials such as cubes, prisms, stars, rods etc. [7–10] determine the enhancement of photon yield due to the oscillating dipoles in S-conduction band. These oscillating dipoles which are influenced by the local electro-magnetic fields result in boosting the third-order nonlinear optical susceptibility [7,8]. As the diameter of these nanowires approach the 10–40 nm range, the surface Plasmon wave experiences dielectric confinement which strongly support the nonlinear absorption processes such as single (saturable absorption, SA) and multi-photon absorptions (reverse saturable absorption, RSA) [11]. Amongst several materials investigated thus far (shape based Plasmonic nanomaterials) in NLO studies, Ag nanowires are one of the promising materials due to their exceptional optical properties directing to the well-known applications such as optical switching [11], and optical limiting [12,13]. Multi-dimensional applications of Ag NWS made them very special in the recent day scientific advancement. Very recently, Lei et al. [14] reported on the usage of transparent Ag Nanowires as energy storage

* Corresponding author.
** Corresponding author.
E-mail addresses: soma_venu@uohyd.ac.in (S.V. Rao), gopalakrishna.podagatlapalli@gitam.edu, satgurusai.gk@gmail.com (G.K. Podagatlapalli).

https://doi.org/10.1016/j.optmat.2019.109305
Received 22 May 2019; Received in revised form 3 August 2019; Accepted 7 August 2019

windows. Wu et al. [15] reported on the production of transparent electromagnetic interference shielding (EMI Shielding) silver nanofibers which were produced at room temperature. Other pioneers of the field extensively worked on dimensionality of the nanomaterials and they were able to demonstrate significant properties and usages of silver based 2D materials [16–18]. Further, in the close vicinity of the nanowires on the substrate, Plasmonic hotspots are created providing large evanescent fields and, thereby, an enhancement in the NLO response.

The third-order NLO properties of plasmonic nanoparticles dispersed or embedded in various dielectric matrices has been explored in the regions near/far to the surface plasmon resonance (SPR) band [19,20]. The dispersed plasmonic nanoparticles in a dielectric host provide large third order NLO response than in the solution form [21–23]. Over the last couple of decades, the third order NLO behavior of plasmonic nanoparticles in different dielectric hosts such as silica [24], Al_2O_3 matrix [25–27], ITO [28] were investigated by various researchers and obtained $\chi^{(3)}$ values in a range of 10^{-6}-10^{-9} e.s.u. using nanosecond laser pulses. Torres et al. [29] reported $\chi^{(3)}$ value of one order more ($\sim 10^{-9}$ e.s.u.) in the case of Au NPs and Si quantum dots in SiO_2. Thus obtained $\chi^{(3)}$ values were large compared to the third order nonlinear susceptibility of standard sample CS_2 ($\sim 10^{12}$ e.s.u.) recorded with nanosecond pulses. Moreover, broadband femtosecond (fs) NLO properties of plasmonic nanoparticles (Au, Ag) in SiO_2 matrix have been executed by diverse research groups [30,31]. Though there are many reports available on the NLO studies of silver nanomaterials of different shapes, Ag NWs are less investigated materials by the researchers. We believe that the silver nanowires generate higher number of hotspots compared to aggregated silver nanoparticles. Consequently, fs NLO studies of Ag NWs films on a glass substrate were attempted by us. In this work, we present results of nonlinear absorption (NLA) and nonlinear refraction (NLR) studies of Ag NWs dispersed on a glass host (ordinary cover slip) using a simple technique of Z-scan at different wavelengths 700 nm, 750 nm, 800 nm, 850 nm and 900 nm, using femtosecond (fs) pulses. Furthermore, peak intensity dependent studies of Ag NWS films in open aperture Z-scan method were also performed [32].

2. Experimental details

Silver nanowire suspensions (Ag NWS) in 0.5% isopropanol (IPA) whose dimensios are 60(± 10) nm × 10(± 5) μm, density- 0.785 gm/mL were purchased from Sigma Aldrich (product no-739421, CAS-7440224) and the suspensions posses a thick gray coloration. Prior to the experiment, Ag NWS were sonicated to avoid the agglomeration and to maintain the monodispersionality. Ag NW films were prepared by drop cast method wherein 20 μL solution was utilized and the films were allowed to dry for sometime. While preparing the Ag NWS films, significant transmission of laser beam through the film was ensured by preparing the films with large quantity of solution (> 20 μL). It was found that the quantity 20 μL is an optimal amount of Ag NW colloidal solution to prepare Ag NWs films with required transparancy (70–80%). We performed two studies, **i)** Ag NW films were utilized to investigate optical nonlinear (NLO) properties of the Ag NWs using femtosecond laser pulses of time length 150 fs (Chameleon, 76 MHz, central wavelength of 800 nm) both in the open aperture and closed aperture Z-scan methods [32–34] at 700 nm, 750 nm, 800 nm, 850 nm, and 900 nm at a peak intensity of ~190 MW/cm^2 **ii)** at 800 nm, intensity dependent Z-scan studies were performed at different peak intensities of ~190 MW/cm^2, ~210 MW/cm^2, ~260 MW/cm^2. Complete details of the experimental setup can be found in some of our earlier works [35,36]. Z-scan studies were performed by focusing the input beam with ~4 mm diameter using a lens (f = 10 cm). The estimated beam waist at the focus was ~25 μm. In the wavelength dependent studies, typically ~19 mW of input power (corresponding to 0.27 nJ energy) was utilized where as for the peak intensity dependent studies the utlized input powers were ~19 mW, ~21 mW and ~26 mW. Ag NW film on a glass substrate in a sample holder was kept perfectly normal to the incoming laser beam. Ag NW films were scanned in the focal plane of the lenses within a range of $-10Z_0$ to $+10Z_0$, where Z_0 is the Rayleigh range of the focussed laser beam. The input laser beam was allowed to pass through Ag NWS film and the transmitted light was investigated by a thermal power sensor connected with a power meter. The translational stage and photodiode were interfaced to a computer using LabVIEW software. The transmission curves obtained in both open and closed aperture Z scans were fitted with the theoretical formulae and from the fitting parameters the NLA and the NLR coefficients were estimated. For a bare cover slip (without any nanowire film), no NLO behaviour was observed and was confirmed from the Z-scan studies.

3. Results & discussion

Ag NWs in isopropyl alchol (IPA) were purchased from Sigma Aldrich were kept in a clean and cool area to avoid the contamination due to light exposure. Concentration of the Ag NWs colloids was decreased by mixing them in pure IPA to avoid the saturation in the absorbance. Prior to the dilution Ag NWs in IPA has a dark gray coloration. AgNWs were characterized by UV absorption spectrometer. Fig. 1 shows the recorded UV absoption spectrum of Ag NWs in IPA. In Fig. 1 broad peak is the SPR peak and the sharp peak obtained is from interband transitions in Ag [37]. In general, interband transitions demonstrate their characterstic peak in the UV region. The broad peak in the UV-absorption spectrum is from the intraband transitions wherein conduction electrons in lower energy levels uplift to higher levels of condution band. The FWHM of the UV–Visible absorption peak demonstrate the mono dispersive nature of Ag NWs. The surface Plasmon resonance peak's shoulder is extended up to 840 nm in the UV–Visible absorption spectrum which could be due to the combined resonances of Ag NW piles. Later, Ag NWs were characterized by Field Emission Scanning Electron Microscope (FESEM, Ultra 55 from Carl Zeiss) and confirmed their mono-dispersive nature and morphological information. Fig. 2 depicts the FESEM images of Ag NWs in IPA at different magnifications. Fig. 2 confirms the monodispersive Ag NWS with the average dimensions 10 μm length and 60 nm diameter. Additionally, to elucidate the structural properties of Ag NWS we performed the Transmission Electron Microscopic (TEM, FEI Technai, G2 S-Twin 200 keV) analysis (the data of which is depicted Fig. 3). We performed the selected area electron diffraction (SAED) and high resolution TEM analysis also. SAED pattern [Fig. 3 (b)] demonstrated the single

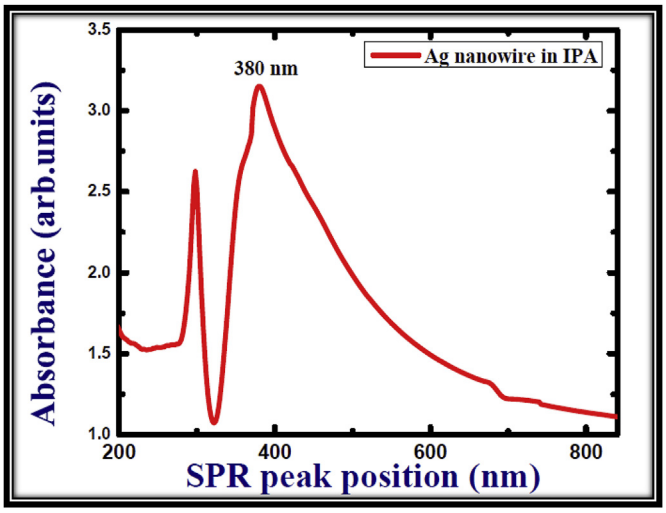

Fig. 1. UV–Vis absorption spectrum of Ag NWs in IPA demonstrating a localized surface Plasmon resonance at 380 nm. Absorbance is measured in arbitrary units.

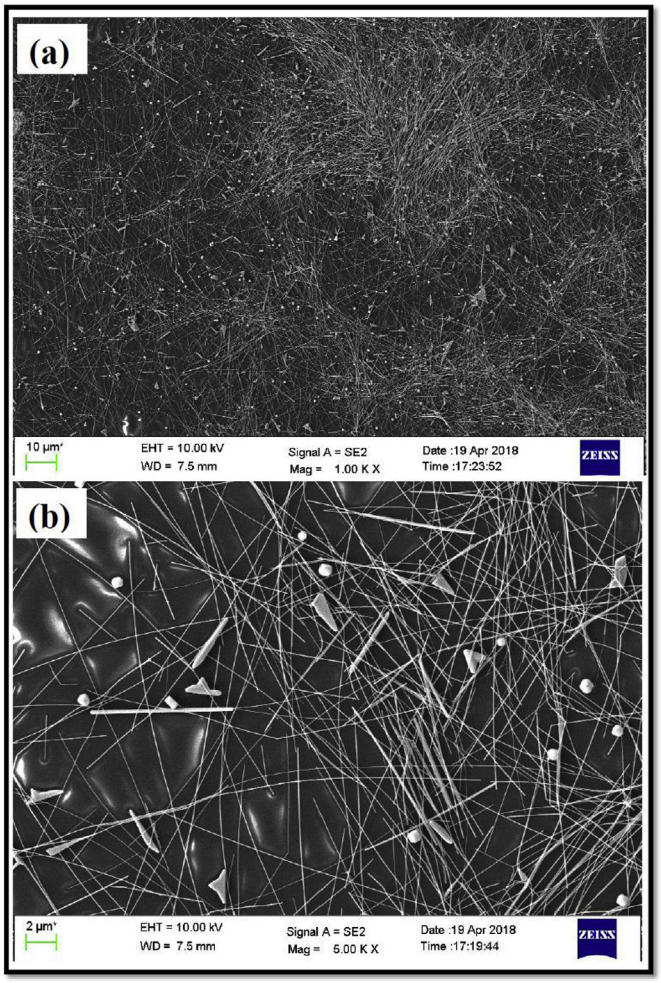

Fig. 2. Field Emission Scanning Electron Microscopic images of Ag NWS taken at the magnifications (a) 10 µm (b) 2 µm to confirm the morphology of silver nanowires and their mono dispersive nature.

crystalline structure of Ag NWS. HRTEM data [Fig. 3(c)] revealed the measured interplanar spacing to be ~0.23 nm, which is in good agreement with the interplanar spacing of [111] lattice plane of silver. The interplanar distance which was obtained from the SAED measurements (0.23 nm) is in good agreement with the face centered cubic (FCC) structure of silver and the corresponding plane is (111). The obtained labelling of [111] for 0.23 nm is in good agreement with PCPDF file no 01–1167 [38,39]. In the determination of lables of each bright spot in SAED pattern, (011) was taken as the zone axis.

To study the NLO properties of Ag NWs on the glass substrate, the transmission Z-scan measurements were carried out. Wavelength dependent optical nonlinearities in Plasmonic materials are of more interest owing to the possibility of potential applications in frequency multiplexing concept. This could be the hypothesis that Plasmonic nanomaterials exhibit strong nonlinear absorption behavior at resonance (or) near the resonance of LSPR wavelength and these studies has been performed by another group recently [10]. In our work, wavelength dependent NLO properties of Ag NWs have been studied near and far-off to the LSPR resonance. Fig. 4 shows the open aperture curves of Ag NWs film substrate recorded at different wavelengths (a) 700 nm, (b) 750 nm, (c) 850 nm, (d) 900 nm at a peak intensity of 190 MW/cm^2 (Open aperture Z-Scan trace of Ag NW film at 800 nm wavelength at a peak intensity of 190 MW/cm^2 is shown in Fig. 5). Error bars in Fig. 4 are of 2% variation in the data points which is due to the fluctuation in the input laser energy. During these studies it was ensured that the average power that was taken at the mentioned wavelengths is more or less same to give a peak intensity of ~190 MW/cm^2. At the input wavelength 700 nm, Ag NWs demonstrated saturable absorption (SA) behavior, characterized by negative nonlinearity whereas RSA in SA (switching behavior was observed at 850 nm and 900 nm. SA and switching (RSA in SA) behaviors are one photon (1 PA) process and TPA with SA process, respectively. When the Ag NWs get excited at 700 nm, the charge transfer possibly takes place from S-band to P-band in the conduction band and finally the S-conduction band has been bleached at lower intensity. Consequently, no more electrons can be moved from S-band to further level and hence Ag NWs exhibited high transparency (SA) near to the focal region. Similarly, ground state bleaching in S-band might occur due to the residual absorption at the excitation of 850 nm and 900 nm at lower intensity and a small dip was observed at focal point which is due to excited state (or) free carrier absorption. In this case, saturation intensity and effective two-photon absorption coefficient have been estimated by using equation (1).

$$\alpha(I) = \frac{\alpha_0}{1 + \frac{I}{I_S}} + \beta I \tag{1}$$

Additionally, for the wavelength of 750 nm, outcome demonstrated reverse saturable absorption (RSA), described by positive β which also could be due to strong quadrupole Plasmon resonance absorption (380 nm) at TPA wavelength. The estimated NLO coefficients are $I_S = 30$ MW/cm^2 ($\beta_{sa} = 0$), $\beta_{TPA} = 1.6 \times 10^{-5}$ cm/W, $I_S = 92$ MW/cm^2 ($\beta_{eff} = 1.4 \times 10^{-5}$ cm/W) and $I_S = 60$ MW/cm^2 ($\beta_{sa} = 1.72 \times 10^{-5}$ cm/W) for the wavelengths of 700 nm, 750 nm, 850 nm and 900 nm, respectively.

Open aperture Z-scan trace at 800 nm is symmetric with respective to zero point (beam waist at the focus), where it demonstrated a dip. This curve revealed that Ag NWs on glass substrate demonstrates pure reverse saturable absorption (RSA). Fitting of the experimental data with the available theoretical formulae for NLA demonstrated that two-photon absorption (TPA) occurred at 800 nm. No NLA behavior was perceived for pure glass substrate at the same intensity utilized in the experiment for the sample. It was confirmed that the nonlinear behavior demonstrated in Fig. 4 is purely accredited to Ag NWs.

Fig. 5 demonstrates nonlinear transmittance exclusive of an open aperture with respect to position of the Ag NW film along the beam propagation direction, at a wavelength of 800 nm for three input peak intensities of ~190 MW/cm^2, ~210 MW/cm^2, ~260 MW/cm^2, corresponding to the input powers ~19 mW, ~21 mW, and ~26 mW, respectively. The fit of equation (3) to the open aperture Z-scan data is illustrated in Fig. 5. The curves in Fig. 4 are fitted with peak intensity dependent absorption coefficient is given by $\alpha(I) = \alpha_0 + \beta \times I$, where α_0 is the linear absorption coefficient, β is the positive nonlinear absorption coefficient (or) two photon absorption coefficient and I is input peak Intensity changes with z (propagation distance). To obtain the theoretical open aperture Z-scan curve [40], it is obligatory to evaluate the below equation

$$\frac{dI}{dZ} = -\alpha(I)I \tag{2}$$

The normalized transmittance open aperture Z-scan equation is mentioned below

$$T_{OA}(Z) = \frac{I_0 \beta L_{eff}}{\left(1 + \left(\frac{Z}{Z_0}\right)^2\right) 2\sqrt{2}} \tag{3}$$

where Z_0 is the Rayleigh range which is related to beam waist ω_0, I_0 is the peak intensity at the focal plane, L_{eff} is the effective length of the sample. Error bars in Fig. 5 are typically 2% variation in the data points which is due to the fluctuation in the input laser energy. The recorded data has been fitted perfectly to two-photon absorption (TPA) coefficient (β) and obtained value was 1.5×10^{-5} cm/W at a peak intensity of 190 MW/cm^2. Earlier investigations demonstrated that the NLO coefficients of various samples are strongly influenced by the

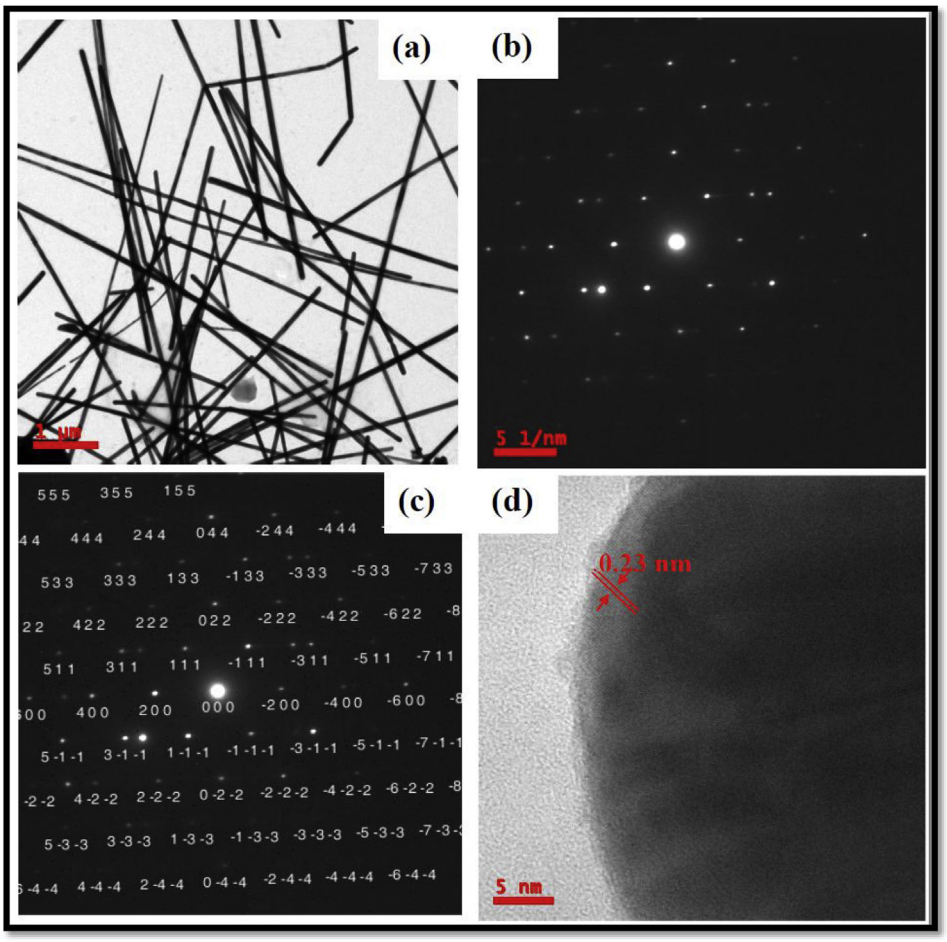

Fig. 3. (a) TEM image of Ag NWS that show the microstructures clearly (b) SAED pattern of Ag NWS which confirms the single crystalline nature of them (c) assignments of various miller indices of lattice planes (d) HRTEM shows the lattice plane s of Ag with an interplanar spacing 0.23 nm which is in agreement with [111] plane of silver.

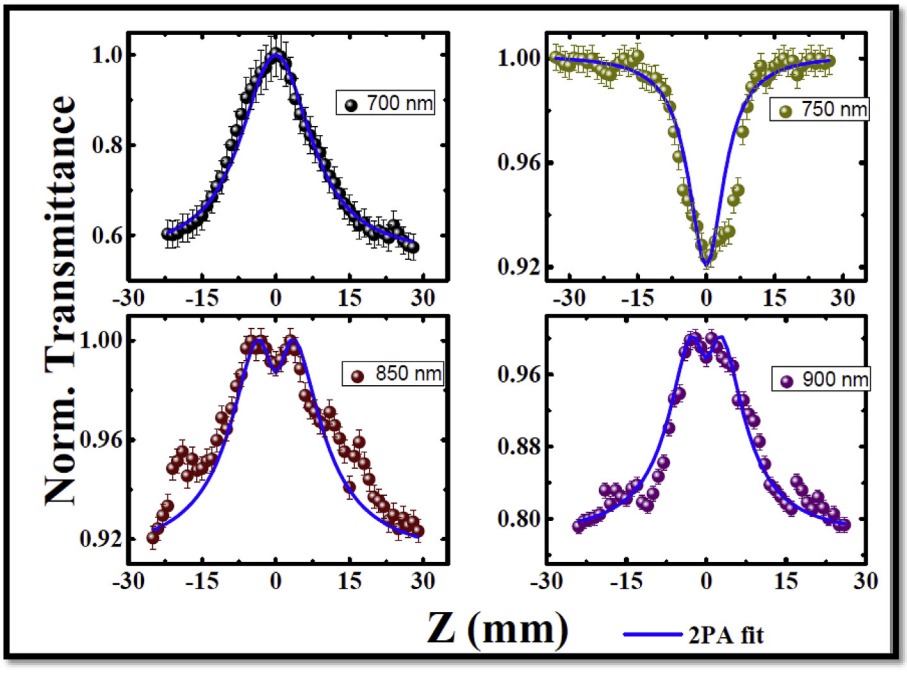

Fig. 4. Open aperture Z Scan curves of Ag NWs film obtained with femtosecond laser pulses with a pulse duration 150 fs at wavelengths (a) 700 nm (b) 750 nm (c) 850 nm and (d) 900 nm. Solid spheres denote the experimental data while the solid lines (blue) represent the theoretical fits. (For interpretation of the references to color in this figure legend, the reader is referred to the Web version of this article.)

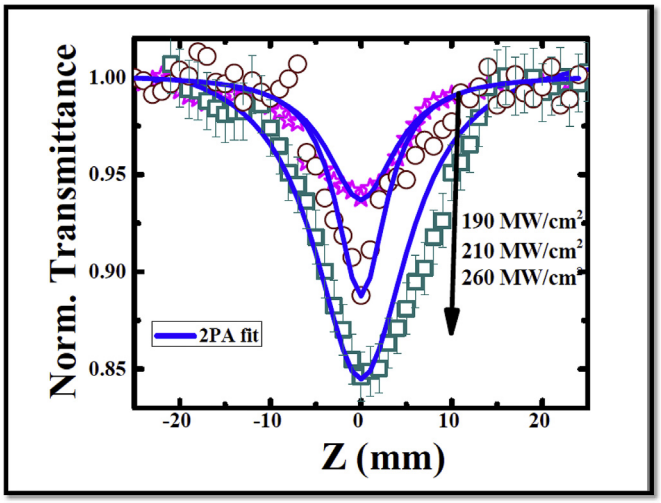

Fig. 5. Open-aperture *Z*-scan data of the Ag NWs film substrate under the excitation of 800 nm with different peak intensities. Open symbols are the experimental data points while the solid curves are theoretical fits.

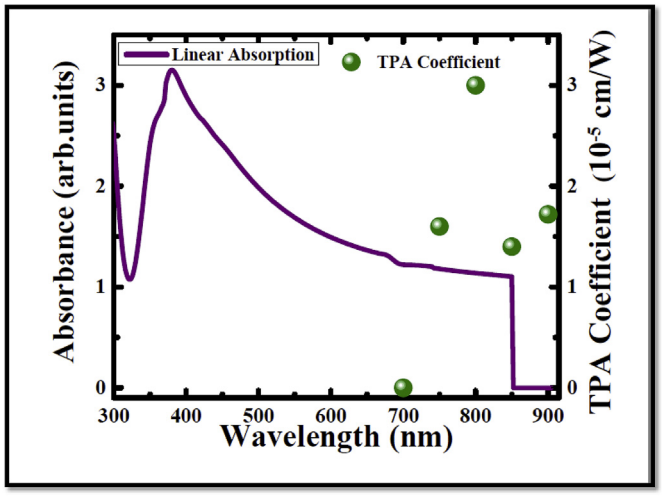

Fig. 6. The obtained two-photon absorption coefficient values (Solid spheres) along with linear absorption spectra (solid line) of the Ag NWs film substrate as a function of wavelength.

fabrication technique, resulting in a big variation in the coefficient values. Hence, expectedly, the values of TPA coefficients are marginally different from the reported values. Wang et al. [11] performed fs NLO studies (76 MHz, 130 fs and 780 nm) of Ag nanowires on polarizing glass prepared by thermal elongation and reduction technology and acquired TPA coefficient values of 0.82 cm/GW at θ = 0 (where laser polarization is parallel to the Ag nanowire axis) and 0.12 cm/GW at θ = 90 (where laser polarization is perpendicular to the Ag nanowire axis). They reported that small TPA coefficient obtained due to laser excitation wavelength is far away from the transverse resonant plasmon peak (θ = 90) and alternatively high TPA value acquired due to relatively strong longitudinal resonance absorption at laser fundamental wavelength. They additionally expressed that the thermal effects were minimized because the samples excited by the laser pulses with weak peak intensity. In our case, we determined the large β (TPA) value could be attained from strong quadrupole plasmon resonance absorption (380 nm) at TPA wavelength and small residual absorption at fundamental wavelength and local evanescent field enhancement owing to electronic transitions from s-band to p-band (or) free carrier absorption. The data presented in Fig. 5 clearly suggests that dip in transmittance increased with peak intensity and obtained coefficients were 3×10^{-5} cm/W and 3.5×10^{-5} cm/GW at peak intensities of 210 MW/cm^2 and 260 MW/cm^2, respectively. It is observed that the β (TPA) value increased as the input peak intensity value is increasing which could be due to excited state absorption (ESA) support the population in ground state massively, thus causing ESA coefficient value be influenced by input fluence. We cannot consider the β values obtained at higher peak intensities to be true TPA coefficients since we expect contributions from higher-order nonlinearities, which was evident from the intensity dependent studies. Even though the pulse duration used was ~150 fs there could be small contributions from excited states to the overall nonlinear transmittance at higher peak intensities. The theoretical fits to the Z-scan experimental data at higher peak intensities were also not ideal. Further detailed studies are warranted to understand the complex behavior at higher peak intensities. Particularly at 800 nm wavelength, the hot spots generated between the piles of silver nanowires might affect the nonlinearities (TPA) and hence the magnitude could have been enhanced. Fig. 6 illustrates the obtained TPA coefficient values along with linear absorption spectra of the Ag NWs with respect to wavelength. It was observed from the results that the highest nonlinear TPA coefficient (β) is acquired at non-resonant absorption peak (800 nm) which does not relate to residual absorption at 800 nm and this could be probably due to the two-photon

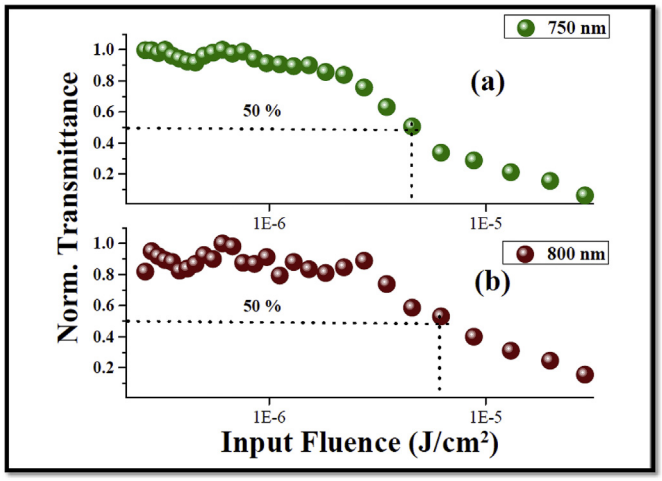

Fig. 7. Optical limiting response of the Ag NWs film substrate obtained at different wavelengths (a) 750 nm and (b) 800 nm.

absorption wavelength quadruple resonance, and it might influence the nonlinear absorption at other different wavelengths. The optical limiting plot for Ag NWs at 750 nm and 800 nm wavelengths is shown in Fig. 7. It was observed that the optical limiting threshold value was considerably small at 750 nm (4.5 μJ/cm^2) compared with 800 nm wavelength (6.2 μJ/cm^2) which could be owing to the strong quadruple resonance at two-photon absorption wavelength. Thermal effects are expected to play an important role in the large NLO coefficients observed in the present case. Though the pulse duration was ~150 fs the high repetition rate will play a significant role in the thermal processes and experimental data obtained with kHz repetition rate pulses will be devoid of any such thermal effects. Our future endeavor will be to record the Z-scan data with kHz fs pulses.

Fig. 8 illustrates the closed aperture Z-scan data of Ag NWs film substrate at different wavelength of (a) 700 nm, (b) 750 nm (c) 800 nm (d) 850 nm and (e) 900 nm, at a peak intensity of 0.05 GW/cm^2. In this characterization, the transmittance of a central portion of Gaussian beam which passes through small sized aperture (S = 0.4) in the far field is recorded. The normal transmittance curve in closed aperture Z-scan was fitted with equation (4)

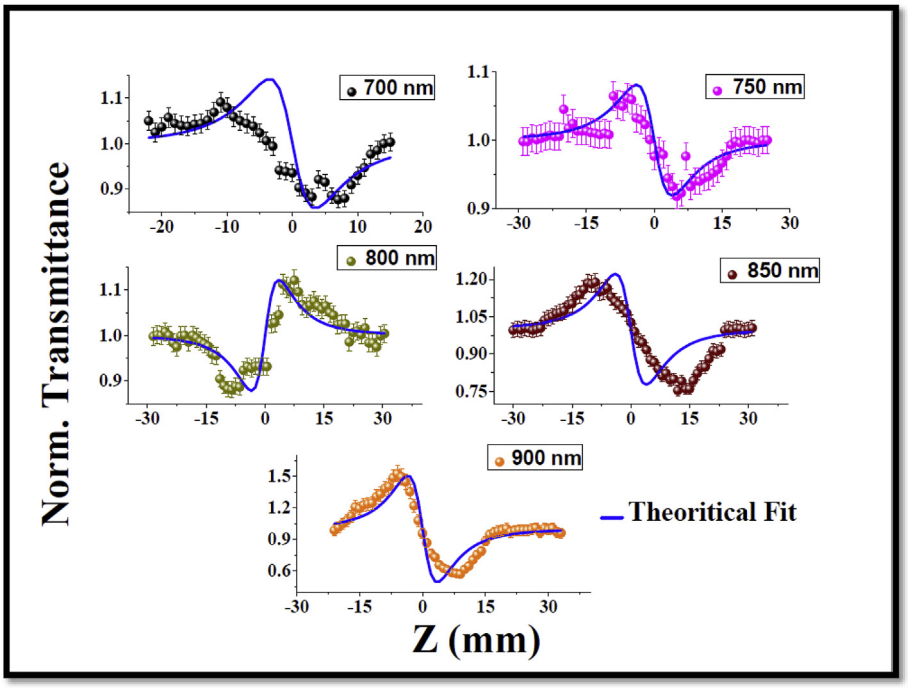

Fig. 8. Closed aperture Z-Scan curves of Ag NWs films obtained with femtosecond laser pulses with a pulse duration 150 fs at wavelengths of (a) 700 nm (b) 750 nm (c) 800 nm (d) 850 nm, and (e) 900 nm. Solid spheres denote the experimental data while the solid lines (blue) represent the theoretical fits. (For interpretation of the references to color in this figure legend, the reader is referred to the Web version of this article.)

$$T_{CA}(Z) = \frac{4\left(\frac{Z}{Z_0}\right)\Delta\varphi}{\left[\left(\frac{Z}{Z_0}\right)^2 + 1\right]\left[\left(\frac{Z}{Z_0}\right)^2 + 9\right]} \quad (4)$$

where $\Delta\phi$ is the phase shift experienced by the ultrafast pulse after traversing the nonlinear medium which is related to the nonlinear refractive index n_2, can be described by the following equation $\Delta\phi = k\, n_2 I_0 L_{eff}$. The sign and coefficient of nonlinearity were strongly influenced by the excitation wavelength and Plasmon band of Ag NWs. The obtained nonlinear refractive index coefficients are -1.6×10^{-9} cm^2/W, -0.9×10^{-9} cm^2/W, 1.6×10^{-9} cm^2/W, is -2.2×10^{-9} cm^2/W, and -19×10^{-9} cm^2/W at wavelength of 700 nm, 750 nm, 800 nm, 850 nm and 900 nm, respectively. Error bars in Fig. 8 are representative of ~2% variation in the data points which is due to fluctuations in the input laser energy. There are two phenomena that explain the nonlinear refractive index curves, including electronic contribution (Kerr effect) and thermal contribution. Thermal effects are predominant when the laser excitation intensity is strong and high repetition rate of ~80 MHz through an increase in the sample temperature. In our experiment, there could be insignificant thermal effects arising from the low peak intensity (0.05 GW/cm^2) but the repetition rate might induce thermal nonlinearities. We believe that the prominent response of nonlinearity in the case of Ag NWs film substrate is electronic nonlinearity (input pulse duration of 150 fs) though the thermal contribution cannot be ruled out. In our present study, the trend of nonlinear coefficients obtained are in good agreement with the previously reported NLO studies of silver nanowires embedded in different hosts, wherein they explained saturable absorption, reverse saturable absorption and the sign of intensity dependent refractive index [41–45]. Further detailed experiments with kHz repetition rate pulses will depict the true electronic nonlinearity and will be a subject of our future investigations.

4. Conclusions

In summary, Ag NWS films prepared by drop cast method were utilized to investigate the NLO behavior of Ag NWS at 700 nm, 750 nm, 800 nm, 850 nm, and 900 nm using both open aperture and closed aperture Z-scan studies. At 800 nm, nonlinear absorption demonstrated pure RSA behavior with a TPA coefficient of ~10^{-5} cm/W. Particularly at 800 nm, nonlinear absorption studies at different peak intensities demonstrated a significant enhancement in the two-photon absorption coefficient. The obtained nonlinear refractive index coefficients are -1.6×10^{-9} cm^2/W, -0.9×10^{-9} cm^2/W, 1.6×10^{-9} cm^2/W, is -2.2×10^{-9} cm^2/W, and -19×10^{-9} cm^2/W at wavelength of 700 nm, 750 nm, 800 nm, 850 nm and 900 nm, respectively. We believe that the retrieved high NLO coefficients might be due to the high density of hot spots those generated between the piles of Ag NWs.

Acknowledgements

Dr. G Krishna Podagatlapalli wishes to acknowledge ACRHEM, University of Hyderabad, for giving permission to carry out the presented research work. S. Venugopal Rao thanks DRDO for continued financial support. S. Venugopal Rao also thanks Centre for Nanotechnology (CFN), University of Hyderabad for the TEM data.

References

[1] J.F. Lamère, P.G. Lacroix, N. Farfán, J.M. Rivera, R. Santillan, K. Nakatani, Synthesis, characterization and nonlinear optical (NLO) properties of a push–pull bis-boronate chromophore with a potential electric field induced NLO switch, J. Mater. Chem. 16 (2006) 2913–2920 https://doi.org/10.1039/B606359D.
[2] S. Kawata, H.-B. Sun, T. Tanaka, K. Takada, Finer features for functional micro devices, Nature 412 (2001) 697–698 https://doi.org/10.1038/35089130.
[3] D. Cotter, R. Manning, K. Blow, A. Ellis, A. Kelly, D. Nesset, I. Phillips, A. Poustie, D. Rogers, Nonlinear optics for high-speed digital information processing, Science 286 (1999) 1523–1528 https://doi.org/10.1126/science.286.5444.1523.
[4] S. Harilal, C. Bindhu, V. Nampoori, C. Vallabhan, Optical limiting and thermal lensing studies in C_{60}, J. Appl. Phys. 86 (1999) 1388–1392 https://doi.org/10.1063/1.370899.
[5] M.A. Kramer, W.R. Tompkin, R.W. Boyd, Nonlinear-optical interactions in fluorescein-doped boric acid glass, Phys. Rev. A 34 (1986) 2026 https://doi.org/10.1103/PhysRevA.34.2026.
[6] F.E. Hernández, A.O. Marcano, Y. Alvarado, A. Biondi, H. Maillotte, Measurement of nonlinear refractive index and two photon absorption in novel organometallic compound, Opt. Commun. 152 (1998) 77 https://doi.org/10.1016/S0030-4018(98)00153-9.
[7] E.V. García Ramírez, S.A. Sabinas Hernández, D. Ramírez Martínez, G. Díaz, J.A. Reyes Esqueda, Third order nonlinear optics in Ag nano cubes: local and nonlocal optical responses as a function of excitation wavelength and particle size, Opt. Express 25 (2017) 31064–31076 https://doi.org/10.1364/oe.25.031064.
[8] A.I. Zvyagin, A.S. Perepelitsa, M.S. Lavlinskaya, O.V. Ovchinnikov, M.S. Smirnov, R.A. Ganeev, Demonstration of variation of the NLO absorption of non-spherical silver nanoparticles, Optik - International Journal for Light and Electron Optics 175

(2018) 93–98 https://10.1016/j.ijleo.2018.08.117.
[9] Y. Hua, K. Chandra, D. Hieu, M.D. Gary, P. Wiederrecht, T.W. Odom, Shape-dependent NLO properties of anisotropic gold nanoparticles, J. Phys. Chem. Lett. 6 (2015) 4904–4908 https://doi.org/10.1021/acs.jpclett.5b02263.
[10] H. Sánchez-Esquivel, K.Y. Raygoza-Sánchez, R. Rangel-Rojo, E. Gemo, N. Michieli, B. Kalinic, J.A. Reyes-Esqueda, T. Cesca, G. Mattei, Spectral dependence of nonlinear absorption in ordered silver metallic nanoprism arrays, Sci. Rep. 7 (2017) 5307 https://doi.org/10.1038/s41598-017-04814-2.
[11] Q.Q. Wang, J.B. Han, H.M. Gong, D.J. Chen, X.J. Zhao, J.Y. Feng, J.J. Ren, Linear and NLO properties of Ag nanowire polarizing glass, Adv. Funct. Mater. 16 (2006) 2405–2408 https://doi.org/10.1002/adfm.200600096.
[12] H. Pan, W. Chen, Y.P. Feng, J. Wei, Optical limiting properties of metal nanowires, Appl. Phys. Lett. 88 (2006) 223106 https://doi.org/10.1063/1.2208549.
[13] Y. Han, M. Luo, Q. Wang, J. Wang, X. Gao, Synthesis of silver nanowires and investigation of their optical limiting properties, Adv. Mater. Res. 295–297 (2011) 152–155 https://doi.org/10.4028/www.scientific.net/amr.295-297.152.
[14] S. Lin, H. Wang, X. Zhang, D. Wang, D. Zu, J. Song, Z. Liu, Y. Huang, K. Huang, N. Tao, Z. Lib, X. Bai, B. Li, M. Lei, Z. Yu, H. Wu, Direct spray-coating of highly robust and transparent Ag nanowires for energy saving windows, Nano Energy 62 (2019) 111–116 https://doi.org/10.1016/j.nanoen.2019.04.071.
[15] S. Lin, H. Wang, F. Wu, Q. Wang, X. Bai, D. Zu, J. Song, D. Wang, Z. Liu, Z. Li, N. Tao, K. Huang, M. Lei, B. Li, H. Wu, Room-temperature production of silver-nanofiber film for large-area, transparent and flexible surface electromagnetic interference shielding, npj flexible electronics 6 (2019) 1–8 https://doi.org/10.1038/s41528-019-0050-8.
[16] X. Wang, Y. Cui, T. Li, M. Lei, J. Li, Z. Wei, Recent advances in the functional 2D photonic and optoelectronic devices, Adv. Opt. Mat. 2018 (2018) 1801274 https://doi.org/10.1002/adom.201801274.
[17] W. Liu, M. Liu, Y. Yang, H. Hou1, M. Lei, Z. Wei, CVD-grown MoSe2 with high modulation depth for ultrafast mode-locked erbium doped fiber laser, Nanotechnology 29 (1–6) (2018) 394002 https://orcid.org/0000-0001-9380-2990.
[18] W.J. Liu, M.L. Liu, B. Liu, R.G. Quhe, M. Lei, S.B. Fang, H. Teng, Z.Y. Wei, Nonlinear optical properties of MoS_2-WS_2 heterostructure in fiber lasers, Opt. Express 27 (2019) 6689–6699 https://doi.org/10.1364/OE.27.006689.
[19] T. Cesca, P. Calvelli, G. Battaglin, P. Mazzoldi, G. Mattei, Local-field enhancement effect on the NLO response of gold-silver nano planets, Opt. Express 20 (2012) 4537 https://doi.org/10.1364/oe.20.004537.
[20] R.F. Haglund, Ion implantation as a tool in the synthesis of practical third-order NLO materials, Mater. Sci. Eng. A 253 (1998) 275–283 https://doi.org/10.1016/S0921-5093(98)00736-9.
[21] H. Tsuji, S. Kido, Y. Gotoh, Ishikawa, Negative-ion implanter for powders and its application to nanometer-sized metal particle formation in the surface of glass beads, Rev. Sci. Instrum. 71 (2000) 804–806 https://doi.org/10.1063/1.1150299.
[22] R. Magruder, Y. Li, J. Haglund, C. White, L. Yang, R. Dorsinville, R.R. Alfano, Optical properties of gold nanocluster composites formed by deep ion implantation in silica, Appl. Phys. Lett. 62 (1993) 1730–1733 https://doi.org/10.1063/1.109588.
[23] R. Ganeev, A. Ryasnyansky, A. Stepanov, T. Usmanov, Characterization of NLO parameters of copper- and silver-doped silica glasses at $\lambda =$ 1064 nm, Phys. Status Solidi B 241 (2004) 935–944 https://doi.org/10.1002/pssb.200301947.
[24] K. Fukumi, A. Chayahara, K. Kadono, Au^+-Ion-Implanted silica glass with nonlinear optical property, Jpn. J. Appl. Phys. 30 (1991) L742–L744 https://doi.org/10.1143/jjap.30.l742.
[25] O. Sánchez-Dena, P. Mota-Santiago, L. Tamayo-Rivera, E.V. García-Ramírez, A. Crespo-Sosa, A. Oliver, J.-A. Reyes-Esqueda, Size-and shape-dependent NLO response of Au nanoparticles embedded in sapphire, Opt. Mater. Express 4 (2014) 92–100 https://doi.org/10.1364/ome.4.000092.
[26] F.Z. Henari, A.A. Dakhel, Linear and nonlinear optical properties of gold nanoparticle-Eu oxide composit nanoparticles, J. Appl. Phys. 104 (2008) 033110https://doi.org/10.1063/1.2967711.
[27] R.A. Ganeev, Single-shot reflection z-scan for measurements of the nonlinear refraction of nontransparent materials, Appl. Phys. B Laser Opt. 91 (2008) 273 https://doi.org/10.1007/s00340-008-2951-4.
[28] A.I. Ryasnyansky, B. Palpant, S. Debrus, R.I. Khaibullin, A.L. Stepanov, NLO properties of copper nanoparticles synthesized in indium tin oxide matrix by ion implantation, J. Opt. Soc. Am. B 23 (2006) 1348–1353 https://doi.org/10.1364/josab.23.001348.
[29] C. Torres-Torres, A. López-Suárez, B. Can-Uc, R. Rangel-Rojo, L. Tamayo-Rivera, A. Oliver, Collective optical Kerr effect exhibited by an integrated configuration of silicon quantum dots and gold nanoparticles embedded in ion-implanted silica, Nanotechnology 26 (2015) 295701 https://doi.org/10.1088/0957-4484/26/29/295701.
[30] I. Tanahashi, H. Inouye, A. Mito, Femtosecond NLO properties of Au/SiO_2 composite thin films prepared by a sputtering method, Jpn. J. Appl. Phys. 42 (2003) 3467–3468 https://doi.org/10.1143/jjap.42.3467.
[31] I. Tanahashi, M. Yoshida, Y. Manabe, T. Tohda, S. Sasaki, T. Tokizaki, A. Nakamura, Preparation and NLO properties of Ag/SiO_2 glass composite thin films, Jpn. J. Appl. Phys. 33 (1994) L1410 https://doi.org/10.1043/jjap.33.l410/meta.
[32] M. Sheik-Bahae, A.A. Said, E.W. Vanstryland, High sensitivity, single beam n_2 measurements, Opt. Lett. 14 (1989) 955 https://doi.org/10.1364/ol.14.000955.
[33] S. Venugopal Rao, D. Narayana Rao, J.A. Akkara, B.S. De Cristofano, D.V.G.L.N. Rao, Dispersion studies of non-linear absorption in C_{60} using *Z*-scan, Chem. Phys. Lett. 297 (1998) 491–498 https://doi.org/10.1016/j.cplett.2011.08.021.
[34] M. Yin, H.P. Li, S.H. Tang, Determination of nonlinear absorption and refraction by single Z-Scan experiment, Appl. Phys. B 70 (2000) 587–591 https://doi.org/10.1007/s003409900156.
[35] S. Venugopal Rao, T.S. Prashant, T. Sarma, P.K. Panda, D. Swain, S.P. Tewari, Two photon and three photon absorption in dinapthtoporphecenes, Chem. Phys. Lett. 514 (2011) 98–103 https://doi.org/10.1016/j.cplett.2011.08.021.
[36] S. Hamad, S.P. Tewari, L. Giribabu, S. Venugopal Rao, Picosecond and femtosecond optical nonlinearities of novel corroles, J. Porphyr. Phthalocyanines 16 (2012) 140–148 https://doi.org/10.1142/S108842461200446X.
[37] S. Venugopal Rao, Picosecond nonlinear optical studies of gold nanoparticles synthesised using coriander leaves (Coriandrum sativum), J. Mod. Opt. 58 (2011) 1024–1029 https://doi.org/10.1080/09500340.2011.590903.
[38] E.R. Jette, F. Foote, Precision determination of lattice constants, J. Chem. Phys. 3 (1935) 605–616 https://doi.org/10.1063/1.1749657.
[39] G.K. Podagatlapalli, S. Hamad, M.A. Mohiddon, Effect of oblique incidence on silver nanomaterials fabricated in water via ultrafast laser ablation for photonics and explosive detection, Appl. Surf. Sci. 303 (2014) 217–232 https://doi.org/10.1016/j.apsusc.2014.02.152.
[40] A. Gaur, S. Hamad, Y. Balaji, S. Venugopal Rao, Experimental evidence of two-photon absorption and three-photon absorption in methylene green: a femtosecond Z-scan study, J. Opt. Soc. Am. B 35 (2018) 2906–2914.
[41] Y.P. Han, J.L. Sun·H, A. Ye·W, Z. Wu ·G. Shi, Nonlinear refraction of silver nanowires from nanosecond to femtosecond laser excitation, Appl. Phys. B 94 (2009) 233–237 https://doi.org/10.1007/s00340-008-3333-7.
[42] S. Luo, Y. Chen, G. Fan, F. Sun, S. Qu, Saturable absorption and reverse saturable absorption on silver particles with different shapes, Appl. Phys. A 117 (2014) 891–894 https://doi.org/10.1007/s00339-014-8449-5.
[43] M. Kröll, S.M. O'Flaherty, W.J. Blau, Optical properties of silver nanowires in nanoporous alumina membranes, Proc. SPIE 4876 (2003) 641–648.
[44] H. Wang, L. Miao, Y. Jiang, S. Lu, Z. Li, P. Li, C. Zhao, H. Zhang, S. Wen, Enhancing the saturable absorption and carrier dynamics of graphene with plasmonic nanowires, Phys. Status Solidi B 252 (2015) 2159–2166 https://doi.org/10.1002/pssb.201552172.
[45] C. Zheng, X.Y. Ye, S.G. Cai, M.J. Wang, X.Q. Xiao, Observation of nonlinear saturable and reverse-saturable absorption in silver nanowires and their silica gel glass composite, Appl. Phys. B 101 (2010) 835–840 https://doi.org/10.1007/s00340-010-4164-x.